Robotica (2004) volume 22, pp. 77–84. © 2004 Cambridge University Press
DOI: 10.1017/S0263574703005228 Printed in the United Kingdom

Optimum design of parallel kinematic toolheads with genetic algorithms

Dan Zhang*, Zhengyi Xu†, Chris M. Mechefske‡ and Fengfeng Xi§

(Received in Final Form: May 3, 2003)

SUMMARY

In this paper, the optimum design of parallel kinematic toolheads is implemented using genetic algorithms with the consideration of the global stiffness and workspace volume of the toolheads. First, a complete kinetostatic model is developed which includes three types of compliance, namely, actuator compliance, leg bending compliance and leg axial compliance. Second, based on this model, two kinetostatic performance indices are introduced to provide a new means of measuring compliance over the workspace. These two kinetostatic performance indices are the mean value and the standard deviation of the trace of the generalized compliance matrix. The mean value represents the average compliance of the Parallel Kinematic Machines over the workspace, while the standard deviation indicates the compliance fluctuation relative to the mean value. Third, design optimization is implemented for global stiffness and working volume based on kinetostatic performance indices. Additionally, some compliance comparisons between Tripod toolhead and other two principal Tripod-based Parallel Kinematic Machines are conducted.

1. INTRODUCTION

Since most machining operations only require a maximum of 5 axes, new configurations with less than six parallel axes would be more appropriate. Development work on new configurations is currently focused mainly on tripods. Examples include Triaglide,[1] Tetrahedral Tripod,[2] and Tricept of Neos Robotics.[3] Tripods can be combined with 2 axis systems, such as x-y stages, to form five axis machines.

To scale down the size of tripods, they can be developed as toolheads. As shown, reference [4], tripod-based toolheads can be attached to existing systems such as CNC machines, robots and CMM, to expand their motion range and dexterity. In this paper, a method for design and optimisation of parallel kinematic toolheads is presented. The method includes kinetostatic modelling, and genetic algorithms.

Kinetostatic analysis is essential for parallel kinematic toolheads. A great deal of work has been done on kinetostatic analysis that has direct application to Parallel Kinematic Machines (hereafter PKMs).[5–12] The work done so far on kinetostatic analysis of PKMs, however, has not addressed the issue of how to improve the global stiffness and workspace simultaneously over the workspace. In this paper, two global compliance indices (kinetostatic performance indices) are introduced, namely, the mean value and the standard deviation of the trace of the generalized compliance matrix. The mean value represents the average compliance of the PKM over the workspace, while the standard deviation indicates the compliance fluctuation relative to the mean value. With the two indices, the optimization objective function for both global stiffness and workspace is proposed.

Meanwhile, the analysis of the positioning and orientation error of the platform in the presence of leg flexibility has not received much attention. However, this error cannot be neglected in practice, since it has been shown that if the mechanism flexibility is considered, the performances may become very poor and the main feature of the mechanism is lost. It is shown that it is necessary to take link flexibility into account.[12] The relationship between mechanism global stiffness and link flexibilities is derived in the paper.

Genetic algorithms (hereafter GAs) were introduced in the 1970s[13] as part of the large class of evolutionary algorithms,[14] evolution strategies[15] and genetic programming.[16] GAs are powerful and broadly applicable stochastic search and optimization techniques based on the evolutionary principle of natural chromosomes.[17] Specifically, the evolution of chromosomes due to the operation of crossover and mutation and natural selection of chromosomes based on Darwin's survival-of-the-fittest principles are all artificially simulated to constitute a robust search and optimization procedure. GAs are the computer simulation of such evolution where the user provides the environment (function) in which the population must evolve.

In what follows, firstly the generalized compliance matrix is modelled; secondly the global compliance is defined; thirdly genetic algorithms are introduced to implement the optimization. The proposed method is implemented to perform design optimization of the Tripod toolhead prototype built at the Integrated Manufacturing Technologies Institute of the National Research Council of Canada.

* Integrated Manufacturing Technologies Institute, National Research Council Canada, London, Ontario (Canada) N6G 4X8
† Department of Mechanical and Industrial Engineering, University of Toronto, Toronto, Ontario (Canada) M5S 3G8
‡ Department of Mechanical Engineering, Queen's University, Kingston, Ontario (Canada) K7L 3N6
§ Department of Mechanical, Aerospace and Industrial Engineering, Ryerson University, Toronto, Ontario (Canada) M5B 2K3

2. PROBLEM FORMULATION

2.1. System description

Figure 1 shows the CAD model of the tripod that was developed as a toolhead. The tripod is based on the fixed-length legs. A tool can be mounted on the moving platform of the toolhead. The movement of the moving platform is controlled by sliding the fixed-length legs along the guideways. The toolhead can be mounted on an industrial robot as shown in Figure 2(a), on a horizontal CNC machine as shown in Figure 2(b), on a gantry system as shown in Figure 2(c), and on a CMM laser scanning system as shown in Figure 2(d).[4]

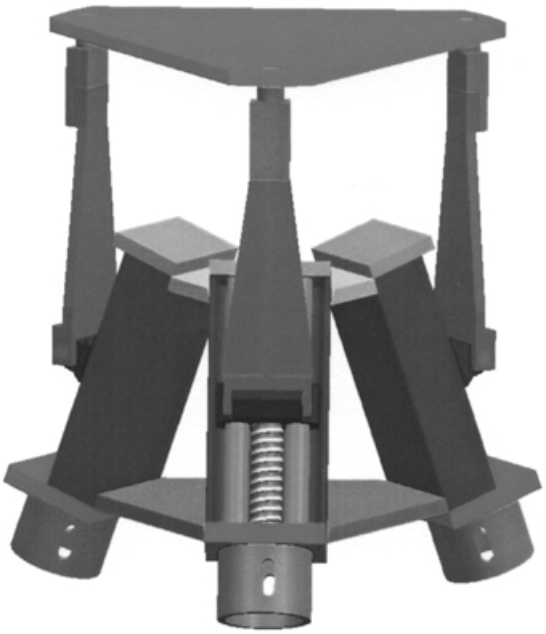

Fig. 1. The CAD model of the tripod toolhead.

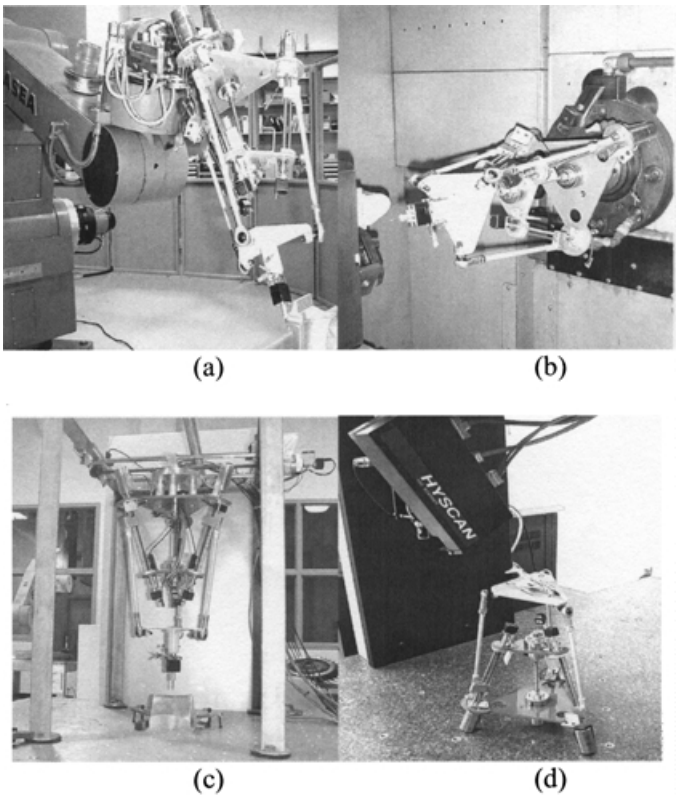

Fig. 2. Various application of Tripod Toolhead.

2.2. Objective function

In this paper, consideration for optimization is to minimize the global compliance and to increase the workspace volume to a certain value. Therefore, it is a multi-objective optimization problem. While implementing the optimisation, we set the workspace volume to a certain increased value, and simply to maximize the global stiffness. The objective function is given as

$$\text{val} = \max(1/\mu + 1/\sigma) \tag{1}$$

where μ represents the mean value of the trace of the global compliance matrix of the tripod, σ is its standard deviation.

The methods for determination of the workspace can be found in the literature and the method used is the inverse kinematics-based method.[18] The global compliance is a new idea that will be introduced in the following section.

3. GENERALIZED STIFFNESS AND COMPLIANCE MATRIX

The generalized stiffness matrix of a PKM relates a wrench including the forces and moments acting on the moving platform to its deformation. It represents how stiff the PKM is in order to withstand the applied forces and moments. By definition, the following relationship holds

$$\mathbf{w} = \mathbf{K}\,\delta\mathbf{x} \tag{2}$$

where $\mathbf{w}$ is the vector representing the wrench acting on the moving platform, $\delta\mathbf{x}$ is the vector of the linear and angular deformation of the moving platform, and $\mathbf{K}$ is the generalized stiffness matrix. Vectors $\mathbf{w}$ and $\delta\mathbf{x}$ are expressed in the Cartesian coordinates *O-xyz*.

Since PKMs are parallel structures, the moving platform stiffness is a combination resulting from all serial chains including actuators. Figure 3 shows a schematic of the Tripod with fixed-length legs. In this type of PKM, the moving platform is driven by sliding the fixed-length legs along the guideways. Three types of compliance contribute to deformation of the moving platform, namely, actuator flexibility, leg bending and axial deformation.

A simple way of deriving the generalized stiffness matrix is to use the force relation and the infinitesimal motion relation as given below in duality form[19]

$$\mathbf{w} = \mathbf{J}^{\mathrm{T}}\mathbf{f} \tag{3}$$

and

$$\delta\mathbf{q} = \mathbf{J}\,\delta\mathbf{x} \tag{4}$$

where $\mathbf{J}$ is the Jacobian matrix that relates the infinitesimal motion between the sub-serial chains and the moving platform, $\mathbf{f}$ is the vector representing forces in the sub-serial chains; $\delta\mathbf{q}$ is the vector representing infinitesimal motion of the sub-serial chains. The infinitesimal motion of the sub-serial chains is referred to as the component deformation in the sub-serial chains. The component deformation would induce the forces, which are called the branch forces in the sub-serial chains.

https://doi.org/10.1017/S0263574703005228 Published online by Cambridge University Press

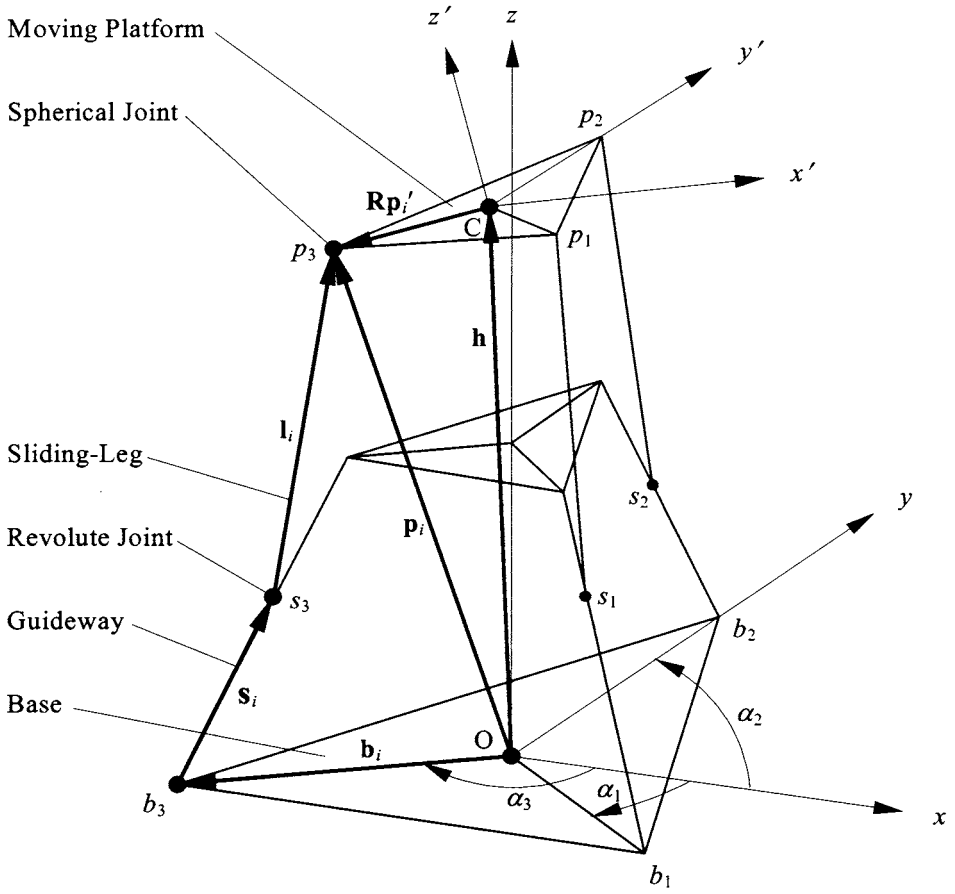

Fig. 3. Schematic of a Tripod Toolhead.

Considering the local stiffness in the sub-serial chains, denoted by $\bar{\mathbf{K}}$, the branch forces induced by the branch deformation can be written as

$$\mathbf{f}=\bar{\mathbf{K}}\,\delta\mathbf{q} \tag{5}$$

Substitution of Equations (4) and (5) into Equation (3) yields

$$\mathbf{w}=\mathbf{K}\,\delta\mathbf{x} \tag{6}$$

where the generalized stiffness matrix $\mathbf{K}$ is given as

$$\mathbf{K}=\mathbf{J}^{\mathrm{T}}\bar{\mathbf{K}}\mathbf{J} \tag{7}$$

Equation (6) can be re-written in terms of compliance as

$$\delta\mathbf{x}=\mathbf{C}\mathbf{w} \tag{8}$$

where $\mathbf{C}$ is the generalized compliance matrix, and $\mathbf{C}=\mathbf{K}^{-1}$. The generalized compliance matrix represents how much the moving platform would deform under the applied wrench $\mathbf{w}$.

When Equation (8) is applied to consider the aforementioned three types of compliance, the following three types of the moving platform deformation would be induced

$$\delta\mathbf{x}_{\mathrm{t}}=\mathbf{C}_{\mathrm{t}}\mathbf{w};\ \delta\mathbf{x}_{\mathrm{b}}=\mathbf{C}_{\mathrm{b}}\mathbf{w};\ \delta\mathbf{x}_{\mathrm{a}}=\mathbf{C}_{\mathrm{a}}\mathbf{w} \tag{9}$$

where subscripts *t*, *b* and *a* indicate the deformation due to the torsion in the actuators, bending and axial deformation of the legs, respectively. Since these three deformations occur in a serial fashion, the total deformation can be considered as follows[20]

$$\delta\mathbf{x}=\delta\mathbf{x}_{\mathrm{t}}+\delta\mathbf{x}_{\mathrm{b}}+\delta\mathbf{x}_{\mathrm{a}} \tag{10}$$

This leads to the following compliance model

$$\delta\mathbf{x}=\mathbf{C}_{\mathrm{G}}\mathbf{w} \tag{11}$$

where the total generalized compliance matrix $\mathbf{C}_{\mathrm{G}}$ is given as

$$\mathbf{C}_{\mathrm{G}}=\mathbf{C}_{\mathrm{t}}+\mathbf{C}_{\mathrm{b}}+\mathbf{C}_{\mathrm{a}} \tag{12a}$$

In Equation (12a), $\mathbf{C}_{\mathrm{t}}=\mathbf{K}_{\mathrm{t}}^{-1}$, $\mathbf{C}_{\mathrm{b}}=\mathbf{K}_{\mathrm{b}}^{-1}$, and $\mathbf{C}_{\mathrm{a}}=\mathbf{K}_{\mathrm{a}}^{-1}$, and Equation (12a) can be re-written as

$$\mathbf{C}_{\mathrm{G}}=\mathbf{K}_{\mathrm{t}}^{-1}+\mathbf{K}_{\mathrm{b}}^{-1}+\mathbf{K}_{\mathrm{a}}^{-1} \tag{12b}$$

where

$$\mathbf{K}_{\mathrm{t}}=\mathbf{J}_{\mathrm{t}}^{\mathrm{T}}\bar{\mathbf{K}}_{t}\mathbf{J}_{\mathrm{t}} \tag{13a}$$

$$\mathbf{K}_{\mathrm{b}}=\mathbf{J}_{\mathrm{b}}^{\mathrm{T}}\bar{\mathbf{K}}_{b}\mathbf{J}_{\mathrm{b}} \tag{13b}$$

$$\mathbf{K}_{\mathrm{a}}=\mathbf{J}_{\mathrm{a}}^{\mathrm{T}}\bar{\mathbf{K}}_{a}\mathbf{J}_{\mathrm{a}} \tag{13c}$$

The total generalized stiffness matrix considering the three types of compliance can be written as

$$\mathbf{K}_{\mathrm{G}}=\mathbf{C}_{\mathrm{G}}^{-1} \tag{14}$$

From Equations (13a)–(13c), it can be seen that CG is defined by three different Jacobians and local stiffness corresponding to three types of compliance, which will be derived in the following section. Though three stiffness matrices $\mathbf{K}_{\mathrm{t}}$, $\mathbf{K}_{\mathrm{b}}$, and $\mathbf{K}_{\mathrm{a}}$ are derived here for the prototype 3-DOF mechanism under study, the method presented is generic and can be readily expanded to PKMs with more than 3 DOF.

However, the total generalized compliance matrix as defined in Equation (12a) does not have the appropriate

https://doi.org/10.1017/S0263574703005228 Published online by Cambridge University Press

units due to multiplication of the Jacobian. For this reason, a weighting matrix is applied to $\mathbf{C}_G$ that becomes

$$\mathbf{C}_W = \mathbf{W}\mathbf{C}_G\mathbf{W} \tag{15}$$

where the weighting matrix is defined as

$$\mathbf{W} = \text{diag}(1, 1, 1, L, L, L) \tag{16}$$

In Equation (16), L is a parameter with length unit. $\mathbf{C}_w$ is a 6×6 matrix with the appropriate compliance units. The upper left 3×3 sub-matrix of $\mathbf{C}_w$ represents the linear compliance with unit of m/N, while the lower right 3×3 sub-matrix represents the angular compliance with unit of rad/Nm. The rest is the coupling between the linear and angular compliance.

As shown in Equation (12b), the compliance matrix is determined by the inverse of the stiffness matrix. Considering Equation (13) and Equation (15), the total generalized compliance matrix can be expressed as

$$\mathbf{C}_W = \mathbf{W}[(\mathbf{J}_t^T\bar{\mathbf{K}}_t\mathbf{J}_t)^{-1} + (\mathbf{J}_b^T\bar{\mathbf{K}}_b\mathbf{J}_b)^{-1} + (\mathbf{J}_a^T\bar{\mathbf{K}}_a\mathbf{J}_a)^{-1}]\mathbf{W} \tag{17a}$$

For the prototype under study it is an over-constrained kinematic system, and three Jacobians $\mathbf{J}_t$, $\mathbf{J}_b$ and $\mathbf{J}_a$ are 3×6 matricides. For this reason, the generalized inverse is applied and Equation (17a) is rewritten as

$$\mathbf{C}_W = \mathbf{C}_{Wt} + \mathbf{C}_{Wb} + \mathbf{C}_{Wa} \tag{17b}$$

where

$$\mathbf{C}_{Wt} = \mathbf{W}\mathbf{J}_t^+\bar{\mathbf{K}}_t^{-1}(\mathbf{J}_t^+)^T\mathbf{W};\ \mathbf{C}_{Wb} = \mathbf{W}\mathbf{J}_b^+\bar{\mathbf{K}}_b^{-1}(\mathbf{J}_b^+)^T\mathbf{W};\ \mathbf{C}_{Wa} = \mathbf{W}\mathbf{J}_a^+\bar{\mathbf{K}}_a^{-1}(\mathbf{J}_a^+)^T\mathbf{W} \tag{18}$$

In Equation (18), superscript + indicates the matrix generalized inverse.

4. STIFFNESS MODELLING AND DERIVATION OF JACOBIANS

4.1. Actuators

Figure 4 shows a schematic of the actuator-leg system in which an actuator drives a fixed-length leg through a lead screw. This design was adopted for our prototype because of cost effectiveness. There exists friction in the lead screw that induces torsional deformation in the actuator shaft and the lead screw itself. The torque, denoted by τ_i, induced by the angular deformation, denoted by $\delta\theta_i$, may be written as

$$\tau_i = k_{\theta i}\,\delta\theta_i \tag{19}$$

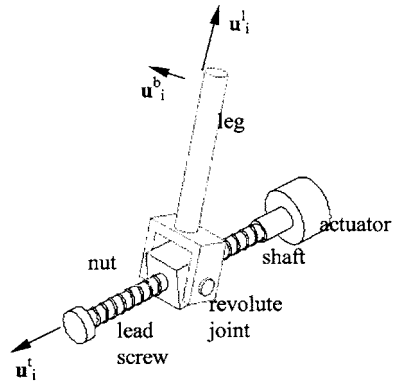

Fig. 4. Actuator and fixed-length leg system.

where $k_{\theta i}$ is the torsional stiffness, i is the branch index, and i = 1, 2, 3 for the prototype under study.

The torque and the rotation of the lead screw can be converted to the force acting on the nut denoted by f_{ti}, and the linear movement of the nut, denoted by δt_i, approximately as[21]

$$f_{ti} = 2\tau_i/(f_c\, d_m); \qquad \delta t_i = p\,\delta\theta_i \tag{20}$$

where f_c is the friction coefficient, d_m is the pitch diameter of the screw and p is the pitch of the screw. Using Equations (19) and (20), the following relationship can be obtained as

$$f_{ti} = k_{ti}\,\delta t_i \tag{21}$$

where k_{ti} represents the stiffness relating δt_i to f_{ti}, and it is given as

$$k_{ti} = 2k_{\theta i}/(f_c\, d_m\, p) \tag{22}$$

Considering all the serial chains, the local stiffness matrix can be expressed as

$$\bar{\mathbf{K}}_t = \text{diag}(k_{ti}) \tag{23}$$

To obtain the generalized stiffness matrix $\mathbf{K}_t$ pertaining to the actuator stiffness, Jacobian $\mathbf{J}_t$ is required. To do so, let us consider the loop equation of the ith branch shown in Figure 3

$$\mathbf{h} + \mathbf{R}\bar{\mathbf{p}}_i - \mathbf{l}_i - \mathbf{t}_i - \mathbf{b}_i = \mathbf{0} \tag{24}$$

where $\mathbf{h}$ and $\mathbf{R}$ are the position vector and the rotation matrix of the moving platform, respectively, $\bar{\mathbf{p}}_i$ is the position vector of joint i on the moving platform in the local coordinates $O' - x'y'z'$, $\mathbf{l}_i$ is the vector representing the ith sliding leg, $\mathbf{t}_i$ is the vector representing the nut displacement along the ith guideway, and $\mathbf{b}_i$ is the position vector of the lower end of the ith guideway. Differentiation of Equation (24) yields[4]

$$\delta\mathbf{t} = \mathbf{J}_t\,\delta\mathbf{x}_t \tag{25}$$

where δt is the vector of the infinitesimal motion of the nut along the guideway, for the prototype under study, $\delta\mathbf{t} = [\delta t_1, \delta t_2, \delta t_3]^T$, and Jacobian $\mathbf{J}_t$ can be obtained as

$$\mathbf{J}_t = \mathbf{B}^{-1}\mathbf{A} \tag{26}$$

In Equation (26), $\mathbf{A}$ and $\mathbf{B}$ are the inverse and forward Jacobian of the PKM and for the prototype under study, they are given as

$$\mathbf{A} = \begin{bmatrix} (\mathbf{u}_1^l)^T & (\mathbf{R}\bar{\mathbf{p}}_1 \times \mathbf{u}_1^l)^T \\ (\mathbf{u}_2^l)^T & (\mathbf{R}\bar{\mathbf{p}}_2 \times \mathbf{u}_2^l)^T \\ (\mathbf{u}_3^l)^T & (\mathbf{R}\bar{\mathbf{p}}_3 \times \mathbf{u}_3^l)^T \end{bmatrix};\quad \mathbf{B} = \text{diag}((\mathbf{u}_1^t)^T\mathbf{u}_1^l, (\mathbf{u}_2^t)^T\mathbf{u}_2^l, (\mathbf{u}_3^t)^T\mathbf{u}_3^l) \tag{27}$$

where $\mathbf{u}_i^t$ and $\mathbf{u}_i^l$ are the unit vectors representing the directions of the ith guideway and the ith leg, respectively. Substituting Equation (23) and (26) into Equation (13a) leads to $\mathbf{K}_t$.

4.2. Fixed-length legs

If the fixed-length leg is connected to the nut by a revolute joint as shown in Figure 4, it would be subject to bending in the direction parallel to the axis of the revolute joint.

https://doi.org/10.1017/S0263574703005228 Published online by Cambridge University Press

Furthermore, since the leg is connected to the moving platform by a spherical joint and assuming there is no friction, the leg can be modelled as clamped (at the revolute joint) – free (at the spherical joint). Under this boundary condition, the following holds

$$f_{bi} = k_{bi}\,\delta b_i \tag{28}$$

where f_{bi} is the force due to the bending deformation δb_i at the free end, and k_{bi} is the bending stiffness given as $k_{bi} = 3EI/l^3$ in which E is the Young's modulus, I is the area moment of leg's cross section, and l is the leg length. If considering all the sub-serial chains, the local stiffness matrix can be obtained as

$$\bar{\mathbf{K}}_b = \mathrm{diag}(k_{bi}) \tag{29}$$

To derive the Jacobian $\mathbf{J}_b$, we can consider $\mathbf{w}$ due to $\mathbf{f}_b = [f_{b1}\ f_{b2}\ f_{b3}]^T$. For the Tripod under study, it can be given as

$$\mathbf{w} = \begin{bmatrix} \mathbf{u}_1^b & \mathbf{u}_2^b & \mathbf{u}_3^b \\ \mathbf{R}\bar{\mathbf{p}}_1 \times \mathbf{u}_1^b & \mathbf{R}\bar{\mathbf{p}}_2 \times \mathbf{u}_2^b & \mathbf{R}\bar{\mathbf{p}}_3 \times \mathbf{u}_3^b \end{bmatrix} \mathbf{f}_b \tag{30}$$

where $\mathbf{u}_i^b$ is the unit vector indicating the bending direction. In the light of the relationship given in Equation (3), $\mathbf{J}_b$ can be obtained from Equation (30) as

$$\mathbf{J}_b = \begin{bmatrix} (\mathbf{u}_1^b)^T & (\mathbf{R}\bar{\mathbf{p}}_1 \times \mathbf{u}_1^b)^T \\ (\mathbf{u}_2^b)^T & (\mathbf{R}\bar{\mathbf{p}}_2 \times \mathbf{u}_2^b)^T \\ (\mathbf{u}_3^b)^T & (\mathbf{R}\bar{\mathbf{p}}_3 \times \mathbf{u}_3^b)^T \end{bmatrix} \tag{31}$$

Substituting Equations (29) and (31) into Equation (13b) gives $\mathbf{K}_b$

In addition to the leg bending, there exists axial deformation along the leg. The force f_{ai} due to the axial deformation δa_i can be given

$$f_{ai} = k_{ai}\,\delta a_i \tag{32}$$

Hence

$$\bar{\mathbf{K}}_a = \mathrm{diag}(k_{ai}) \tag{33}$$

Using a similar approach for the bending, and consider $\mathbf{w}$ due to $\mathbf{f}_a = [f_{a1}\ f_{a2}\ f_{a3}]^T$; it can be readily shown[4]

$$\mathbf{w} = \mathbf{A}^T \mathbf{f}_a \tag{34}$$

Apparently,

$$\mathbf{J}_a = \mathbf{A} \tag{35}$$

Substituting Equations (33) and (35) into Equation (13c) yields $\mathbf{K}_a$.

5. GLOBAL COMPLIANCE INDICES

Indicated by the detailed derivations in Section 4, the generalized compliance matrix $\mathbf{C}_W$ varies over the PKM workspace. Conventional kinetostatic analysis methods, such as stifffiess mapping, would require a large number of graphs in order to provide an overview of the stifffiess variation. An alternative, however, could be based on statistics analysis. This method was proposed to evaluate the generalized mass matrix of PKMs over the workspace.[22] Based on this concept, the mean value and the standard deviation of a selected parameter can be used to evaluate the variation over the workspace. Since the trace of the generalized compliance matrix is invariant, it is selected as a parameter for global kinetostatic analysis. The mean value and the standard deviation are defined as

$$\mu = E(tr(\mathbf{C}_W)) \tag{36}$$

and

$$\sigma = SD(tr(\mathbf{C}_W)) \tag{37}$$

where $E(\cdot)$ and $SD(\cdot)$ are the mean value and the standard deviation, and *tr* represents trace operation. The mean value represents the average compliance of the PKM over the workspace, while the standard deviation indicates the compliance fluctuation relative to the mean value. In general, the lower the mean value the less the deformation, and the lower the standard deviation the more uniform the compliance distribution over the workspace.

6. DESIGN OPTIMIZATION

6.1. Rationale of using genetic algorithms

Genetic algorithms have the advantages of robustness and good convergence properties, i.e.

- They require no knowledge or gradient information about the optimization problems. They can solve any kind of objective functions and any kind of constraints (i.e., linear or nonlinear) defined on discrete, continuous, or mixed search spaces.
- Discontinuities present on the optimization problems have little effect on the overall optimization performance.
- They are effective at performing global search (in probability) instead of local optima.
- They perform very well for large-scale optimization problems.
- They can be employed for a wide variety of optimization problems.

Genetic algorithms have been shown to solve linear and nonlinear problems by exploring all regions of state space and exponentially exploiting promising areas through mutation, crossover, and selection operations applied to individuals in the population.[23]

In the present work, there are many optimization parameters and complex matrix computations. Hence, it is very difficult to write out the analytical expressions for each stifffiess element and workspace volume. Moreover, with traditional optimization methods, only a few geometric parameters could be handled due to the lack of convergence of the optimization algorithm when used with more complex problems.[24] This arises from the fact that traditional optimization methods use a local search by a convergent stepwise procedure (e.g. gradient, Hessians, linearity, and continuity), which compares the values of the next points and moves to the relative optimal points. Global optima can be found only if the problem possesses certain convexity properties that essentially guarantee that any local optima is a global optimum. In other words, Conventional methods are based on point-to-point rule, it has the danger

https://doi.org/10.1017/S0263574703005228 Published online by Cambridge University Press

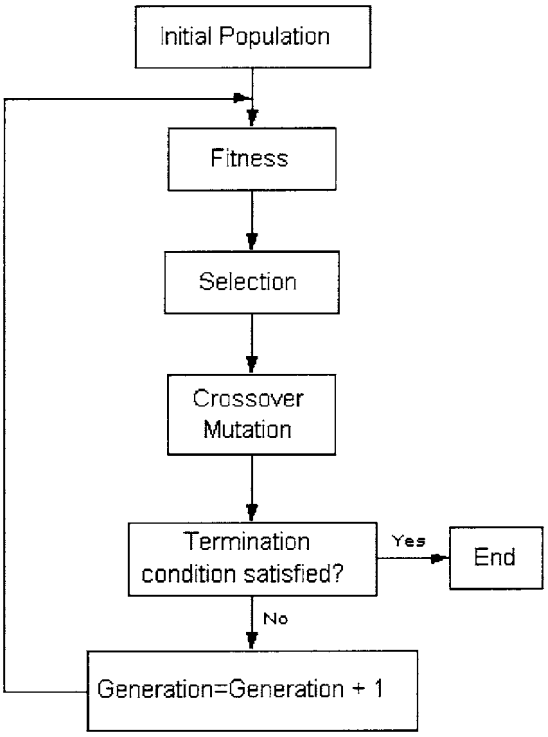

Fig. 5. Genetic algorithms flow chart.

of falling in local optima while the genetic algorithms are based on population-to-population rule, it can escape from local optima. Therefore, genetic algorithms are the best candidate for the optimization problems studied here.

The flowchart of the genetic algorithms is illustrated in Figure 5.

6.2. Determination of parameter settings for Genetic Algorithms

In order to use genetic algorithms properly, several parameter settings have to be determined, they are: chromosome representation, selection function, genetic operators, the creation of the population size, mutation rate, crossover rate, and the evaluation function. They are described in more detail as follows:

- Chromosome representation: This is a basic issue for the GA representation, it is used to describe each individual in the population of interest. For the problem studied here, the chromosomes consist of the architecture parameters (coordinates of the attachment points, coordinates of the moving platform, vertex distributions at base and moving platform, platform height, etc.) and behavior parameters (actuator stifffiess, actuated link stifffiess, etc.) of the mechanisms.
- Selection function: This step is a key procedure to produce the successive generations. It determines which of the individuals will survive and continue on to the next generation. In the paper, the roulette wheel approach is applied.
- Genetic operators: The operators are used to create new children based on the current generation in the population. Basically, there are two types of operators: crossover and mutation. Crossover takes two individuals and produces two new individuals while mutation alters one individual to produce a single new solution.
- Population size: The population size represents the number of individuals or chromosomes in the population.
- Mutation rate: The mutation rate is defined as the percentage of the total number of genes in the population, it determines the probability that a mutation will occur. The best mutation rate is application dependent but for most applications is between 0.001 and 0.1.[23] In the case studied, mutation rate is 0.1.
- Crossover rate: The best crossover rate is application dependent but for most applications is between 0.80 and 0.95.[23] For the case studied, crossover rate is 0.85.
- Evaluation functions: Evaluation functions are subject to the minimal requirement that the function can map the population into a partially ordered set.

7. SIMULATION

7.1. Initialization

Simulations are carried out on the Tripod prototype built at the Integrated Manufacturing Technologies Institute of the National Research Council of Canada as shown in Figure 1. The base platform is a triangular plate with a side length of 245.5 mm and the moving platform is another triangular plate with a side length of 139.7 mm. The guideway length is 95.25 mm and the sliding leg length is 215.9 mm. The guideway angle relative to the vertical direction is 20°. The three stiffness values of the prototype are $k_t = 1.26 \times 10^{10}$ N/m, $k_b = 3.13 \times 10^{10}$ N/m, $k_a = 1.95 \times 10^7$ N/m, and they are the same for the three sub-serial chains.

For the problem studied here, the chromosomes consist of the architecture parameters including coordinates of the attachment points, coordinates of the moving platform, link length, vertex distributions at base and moving platform, platform height etc. Hence, The parameters selected for optimization are: R_p, R_m, h_m, γ, where R_p is the radius of the moving platform; R_m is the radius of the middle plate; h_m is the height of the middle plate with respect to the base plate; γ is the rotation angle of the middle plate with respect to Cartesian Z-axis. And their bounds are

$$R_p \in [60.96, 182.9] \text{ mm}, R_m \in [182.9, 304.8] \text{ mm},$$

$$h_m \in [243.84, 365.76] \text{ mm}, \gamma \in [-\pi/3, 0] \text{ rad}.$$

Some other parameters are set as

$P = 40$,

$G_{max} = 100$.

where P is the population, G_{max} the maximum number of generations.

One can rewrite the objective function Equation (1) as

$$\text{Val}(i) = 1/\mu + 1/\sigma \tag{38}$$

with $i = 1, 2, 3 \ldots 40$.

7.2. Implementation

The objective functions are established and maximized in order to find the suitable geometric parameters (coordinates of the attachment points, coordinates of the moving

https://doi.org/10.1017/S0263574703005228 Published online by Cambridge University Press

platform, link length, vertex distributions at base and moving platform, platform height, etc.) and behaviour parameters (actuator stiffness, actuated link stiffness, and kinetostatic model stiffness, etc.) of the mechanisms. Since the objective function is closely related to the topology and geometry of the structure, and we set the workspace volume to a certain value and to minimize the mean value and standard deviation of the global compliance matrix.

Once the objective function is written, a search domain for each optimization variable (lengths, angles, etc.) should be specified to create an initial population. The limits of the search domain are set by a specified maximum number of generations, since the GAs will force much of the entire population to converge to a single solution.

7.3. Optimization of existing structure

As it is very difficult to optimize global stiffness and workspace to their maximum values simultaneously, as larger workspace always leads smaller stiffness, and vice versa.[25] However, one can solve the problem by determining which item between workspace and stiffness is the dominant one for design and application, and maximize the dominant one while set the other one as a constant (but set as larger than the original). In this research, we set the workspace to a certain value, i.e. the radius of workspace is 304.8 mm, then maximize the global stiffness. The algorithm converged at the 95th generation as shown in Figure 6. The optimized structure parameters are: $[R_p, R_m, h_m, \gamma] = [151, 259.8, 280.5, -0.1762]$, the sum compliance ofthe structure is 0.1568 mm/N.

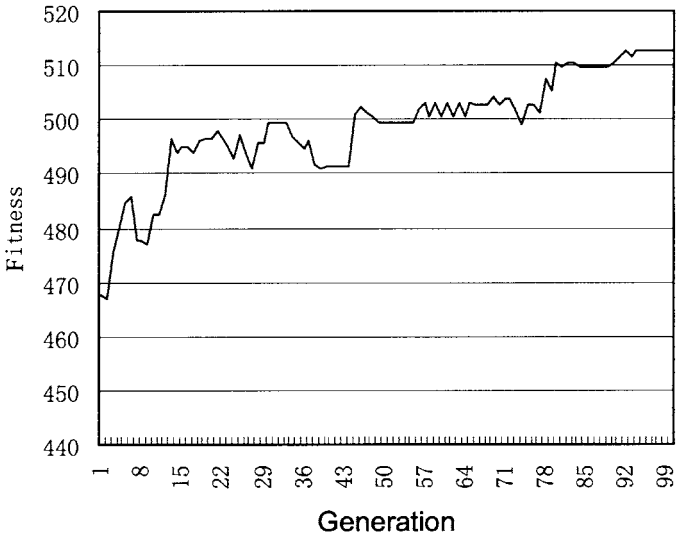

Fig. 6. The evoluation of the performance of the Tripod Toolhead.

Table I shows the comparison before and after optimization, and the global stiffness is apparently improved.

7.3. Comparison of the representative PKM stuctures

Table II is a compliance comparison between the Tripod machine tool and the other two principal PKMs, namely, the Tricept machine tool[26] and Georg V.[27] From the table, one can observe that the optimised Tripod configuration gives a better stiffness among the three parallel kinematic machines

Table I. Optimization results.

	Variable Parameters			Constant Parameters (mm)		Sum Compliance (mm/N)
	R_p (mm)	R_m (mm)	γ (rad)	R_b	D_1	
Initial	60.69	182.88	$-\pi/3$	426.72	20	0.2213
Optimized	151	259.8	–0.1762	462.72	20	0.1568

Table II. Compliance comparison (mm/N)

	TRIPOD				TRICEPT 805				GEORG V			
Height (mm)	Mean value	Standard deviation	max	min	Mean value	Standard deviation	max	min	Mean value	Standard deviation	max	min
210	5.38E-03	0.00E+00	5.38E-03	5.38E-06	7.31E-03	2.85E-06	7.31E-03	7.31E-03	3.06E-03	3.41E-06	3.06E-03	3.06E-03
220	5.44E-03	8.75E-05	5.63E-03	5.34E-03	8.75E-03	8.61E-04	1.07E-02	8.03E-03	3.54E-03	5.02E-05	3.72E-03	3.49E-03
230	5.70E-03	3.09E-04	6.47E-03	5.29E-03	9.60E-03	6.55E-04	1.12E-02	8.81E-03	4.23E-03	2.46E-04	4.95E-03	3.97E-03
240	5.90E-03	5.75E-04	7.67E-03	5.24E-03	1.06E-02	5.79E-04	1.20E-02	9.64E-03	4.85E-03	2.35E-04	5.46E-03	4.51E-03
250	5.78E-03	4.34E-04	6.84E-03	5.20E-03	1.15E-02	6.57E-04	1.34E-02	1.05E-02	5.55E-03	2.75E-04	6.1 8E-03	5.11E-03
260	5.63E-03	3.14E-04	6.30E-03	5.16E-03	1.22E-02	5.12E-04	1.38E-02	1.15E-02	6.20E-03	2.83E-04	7.02E-03	5.79E-03
270	5.48E-03	2.41E-04	6.03E-03	5.12E-03	1.30E-02	3.61E-04	1.41E-02	1.25E-02	6.86E-03	2.15E-04	7.53E-03	6.56E-03
280	5.36E-03	2.17E-04	5.88E-03	5.08E-03	1.39E-02	2.26E-04	1.46E-02	1.35E-02	7.63E-03	1.40E-04	8.07E-03	7.43E-03
290	5.14E-03	8.69E-05	5.35E-03	5.05E-03	1.48E-02	9.97E-05	1.51E-02	1.47E-02	8.53E-03	6.69E-05	8.71E-03	8.44E-03
300	5.02E-03	0.00E+00	5.02E-03	5.02E-03	1.59E-02	1.09E-05	1.59E-02	1.59E-02	9.62E-03	1.12E-05	9.64E-03	9.61E-03
Average	5.48E-03	2.27E-04			1.18E-02	3.97E-04			6.01E-03	1.53E-04		

https://doi.org/10.1017/S0263574703005228 Published online by Cambridge University Press

under the condition of the same geometrical dimensions and actuator stiffness.

8. CONCLUSIONS

It is shown in this paper that the mean value and the standard deviation of the trace of the generalized compliance matrix can not only be used to characterize the kinetostatic behaviour of PKMs globally, but can be used for design optimization. The generalized compliance matrix can be modelled by including three types of compliance, namely, actuator compliance, leg bending and leg axial deformation. The effectiveness of the method has been shown through analyzing the prototype under study. It has been shown that the machine tool workspace and global stiffness can be improved by properly adjusting the geometric configuration.

References

1. H. K. Tonshoff, C. Soehner and H. Ahlers, "A New Machine Tool Concept for Laser Machining", *Proceedings of International Seminar on Improving Machine Tool Performance*, San Sebastian (1998) pp. 199–224,
2. B. S. El-Khasawneh and P. M. Ferreira, "The Tetrahedral Tripod", **In:** *Parallel Kinematic Machines – Theoretical Aspects and Industrial Requirements* (edited by C. R. Boër, L. Molinari-Tosatti and K. S. Smith) (Springer-Verlag, 1999) pp. 419–430.
3. A. Kochan, "Parallel Robots Perfect Propellers", *Industrial Robot* **23**, No. 4, 27–30 (1996).
4. F. Xi, W. Han, M. Verner and A. Ross, "Development of a Sliding-leg Tripod as an Add-on Device for Manufacturing", *Robotica* **19**, Part 3, 285–294 (2000).
5. B. Dasgupta and T. S. Mruthyunjaya, The Stewart Platform Manipulator: a Review, *Mechanism and Machine Theory* **35**, No. 1, 15–40 (2000).
6. H. C. Martin, *Introduction to Matrix Methods of Structural Analysis* (McGraw-Hill Book Company, 1966).
7. C. K. Wang, *Matrix Methods of Structural Analysis* (International Textbook Company, 1966).
8. D. R. Kerr, "Analysis and Design of Stewart-platform Transducer", *ASME Journal of Mechanisms, Transmissions and Automation in Design* **111**, 25–28 (1989).
9. C. M. Gosselin, "Stiffness Mapping for Parallel Manipulators", *IEEE Transaction on Robotics and Automation* **6**, No. 3, 377–382 (1990).
10. B. S. El-Khasawneh and P.M. Ferreira, "Computation of Stiffness and Stiffness Bounds for Parallel Link Manipulators", *Int. J. Machine Tools and Manufacture* **39** 321–342 (1999).
11. F. Tahmasebi, "Kinematic Synthesis and Analysis of a Novel Class of Six-DOF Parallel Minimanipulators", *Ph.D. Thesis* (University of Maryland, 1993).
12. D. Zhang, "Kinetostatic Analysis and Optimization of Parallel and Hybrid Architectures for Machine Tools", *Ph.D. Thesis* (Laval University, Quebec, 2000).
13. J. H. Holland, *Adaptation in Natural and Artificial Systems* (The University of Michigan Press, 1975).
14. L. J. Fogel, A. J. Owens and M. J. Walsh, *Artificial Intelligence Through Simulated Evolution* (John Wiley & Sons, 1966).
15. L. Rechenberg, *Evolutionsstrategie: Optimierun Technischer Systeme nach Prinzipien der Biologischen Evolution* (Frommann-Holzboog, Stuttgart, 1973).
16. J. R. Koza, "Evolving a computer program to generate random numbers using the genetic programming paradigm", *Proceedings of 4th Int. Conf. on Genetic Algorithms* (1991) pp. 37–44.
17. D. Goldberg, *Genetic Algorithms in Search, Optimization and Machine Learning* (Addison-Wesley, 1989).
18. O. Masory and J. Wang, "Workspace evaluation of Stewart platforms", *Advanced Robotics* **9**, No. 4, 443–461 (1995).
19. J.-P. Merlet, *Parallel Robots* (Kluwer Academic Publishers, 2000).
20. William T. Thomson, *Theory of Vibration with Applications* (Prentice Hall, 1993)
21. R. J. Eggert, "Power Screws", *Standard Handbook of Machine Design* (Eds. J. E. Shisley and C. R. Mischke) (McGraw-Hill, 1986).
22. F. Xi, R. Sinatra and W. Han, "Effect of leg inertia on dynamics of sliding-leg hexapods", *ASME Journal of Dynamic Systems, Measurement, and Control* **123**, No. 2, 265–271 (2000).
23. Z. Michalewicz, *Genetic Algorithms + Data Structures = Evolution Programs*, AI Series (Springer-Verlag, New York, 1994).
24. C. M. Gosselin and M. Guillot, "The Synthesis of Manipulators with Prescribed Workspace", *ASME Journal of Mechanical Design* **113**, 451–455 (1991).
25. F. Xi, D. Zhang, Z. Xu and C. Mechefske, "A comparison study on tripod units for machine tools", *International Journal of Machine Tools and Manufacture* (to appear).
26. D. Zhang and C. M. Gosselin, "Kinetostatic analysis and design optimization of the Tricept machine tool family", *ASME Journal of Manufacturing Science and Engineenng* **124**, 725–733 (2002).
27. H. K. Tönshoff, R. Grendel and R. Kaak, "Structure and Characteristics of the Hybrid Manipulator Georg V", **In:** *Parallel Kinematic Machines – Theoretical Aspects and Industrial Requirements* (Edited by C. R. Boër, L. Molinari-Tosatti and K. S. Smith) (Springer Publ., **YEAR**) pp. 365–376.

https://doi.org/10.1017/S0263574703005228 Published online by Cambridge University Press